



# Development of films based on quinoa (*Chenopodium quinoa*, Willdenow) starch

Patricia C. Araujo-Farro<sup>a,\*</sup>, G. Podadera<sup>b</sup>, Paulo J.A. Sobral<sup>b</sup>, Florencia C. Menegalli<sup>a</sup>

<sup>a</sup> Department of Food Engineering, DEA/FEA/UNICAMP, P.O. Box 6121, 13083-862, Campinas, SP, Brazil

<sup>b</sup> Department of Food Engineering, ZEA/FZEA/USP, P.O. Box 23, 13635-900, Pirassununga, SP, Brazil

## ARTICLE INFO

### Article history:

Received 10 February 2010

Received in revised form 4 March 2010

Accepted 29 March 2010

Available online 3 April 2010

### Keywords:

Quinoa starch edible films

*Chenopodium quinoa*

Willdenow

Mechanical properties

Response surface methodology (RSM)

## ABSTRACT

The filmogenic solutions (FS) composed of quinoa starch (4.0 g/100 mL) were prepared, containing various concentrations of glycerol (GC; 16.6–33.4 g glycerol/100 g of quinoa starch, dry weight basis) and alkaline pH values (9.7–11.3). To obtain quinoa starch films (QSF), the FS were dried using different temperature/time combinations ( $T^{\circ}\text{C}/\text{h}$ ) denoted as the drying conditions (DC;  $30^{\circ}\text{C}/20\text{ h}$ – $50^{\circ}\text{C}/5\text{ h}$ ). The influence of GC, pH and DC on the mechanical properties and solubility of QSF was evaluated using response surface methodology (RSM). According to the statistical analyses, the optimized conditions corresponded to 21.2 g of glycerol/100 g of quinoa starch, a pH value of 10.7 and  $36^{\circ}\text{C}/14\text{ h}$  for the DC. The films produced under these conditions exhibited superior mechanical properties ( $7.05 \pm 0.37\text{ N}$  puncture force,  $7.56 \pm 0.95\text{ MPa}$  tensile strength, and  $58.14\% \pm 3.16$  elongation at break), low solubility (15.9%), and optimal barrier properties (WVP of  $0.204 \pm 0.012\text{ g mm m}^{-2}\text{ h}^{-1}\text{ kPa}^{-1}$  and oxygen permeability of  $4.34 \pm 1.03\text{ cm}^3\text{ }\mu\text{m m}^{-2}\text{ d}^{-1}\text{ kPa}$ ).

© 2010 Elsevier Ltd. All rights reserved.

## 1. Introduction

Starch, a renewable biopolymer consisting of amylose and amylopectin, is the most commonly used agricultural raw material for edible film manufacture, since it is inexpensive, relatively easy to handle, totally biodegradable and widely available in nature from sources such as cereals, roots, tubers, palms and more recently the rediscovered pseudocereals such as amaranth and quinoa (Araujo-Farro, Podadera, Sobral, and Menegalli, 2006; Colla, Sobral, & Menegalli, 2006). The quinoa seed (*Chenopodium quinoa*, Willdenow) is a small grain ( $\sim 3\text{ mm}$  diameter) found typically in the South American Andean highlands, and is composed of significant amounts of starch (up to 80%), which has an amylose content of  $\sim 10$ – $21\%$  (depending on the variety) and a small starch granule size ( $\sim 1\text{ }\mu\text{m}$ ), characteristics that allow for easier dispersion, which make this starch a promising material for film production (Ahamed, Singhal, Kulkarni, & Pal, 1996). In addition, according to Araujo-Farro et al. (2006), quinoa starch is able to form transparent edible biodegradable films without any previous chemical treatment. On the other hand, in order to increase the workability and flexibility of edible films based on different starches, various plasticizers, usually polyols, have been widely used, glycerol being one of the most preferred and most studied. Glycerol is a hydrophilic plasticizer, and when added at the correct level with respect to the

biopolymer content, can interfere with chain to chain hydrogen bonding and the water solubility of the biopolymer (protein/starch mixtures), a process generally used to improve the mechanical properties of edible films (Sobral, Menegalli, Hubinger, & Roques, 2001; Sothornvit & Krotcha, 2001). Edible plasticized films are thin, flexible materials made from biopolymers and capable of forming a continuous matrix by adding food grade plasticizers. They are usually manufactured by the wet method, which is based on the drying of a film-forming solution or dispersion by casting on a convenient support. Furthermore, the wet process is generally preferred in order to form edible preformed films or to applied coatings directly onto food products (Colla et al., 2006; Guilbert, 2000; Sobral et al., 2001). According to Alcantara, Rumsey, and Krotcha (1998), Jangchud and Chinnan (1999) and Perez-Gago and Krotcha (2000), the barrier and mechanical properties of edible biodegradable films have been shown to improve when the drying temperatures were increased. In all the situations, the results were attributed to structural changes in film morphology. Thus the drying conditions used during the drying process of the filmogenic solution can be considered as an important factor in obtaining homogeneous films, and have a great influence on their performance.

Edible films based on starch from conventional crops and roots have been extensively studied, and several researchers (Averous & Boquillon, 2004; Bader & Goritz, 1994; Follain, Joly, Dole & Bliard, 2005; Garcia, Martino, & Zaritzky, 2000; Lourdin, Della Valle, & Colonna, 1995; Mali, Grossman, Garcia, Martino, & Zaritzky, 2002; Mali, Grossmann, García, Martino, & Zaritzky, 2005; Mali, Sakanaka, Yamashita, & Grossmann, 2005; Muller, Yamashita, & Borges, 2008; Parris, Dickey, Kurants, Moten & Craig, 1997) have reported the

\* Corresponding author. Tel.: +55 19 35214025; fax: +55 19 35214027.

E-mail addresses: [pcaraujof@yahoo.com](mailto:pcaraujof@yahoo.com), [patricia@fea.unicamp.br](mailto:patricia@fea.unicamp.br) (P.C. Araujo-Farro).

characteristics of the materials formed (starch, edible starch films, plasticized or not, chemically modified or not, used alone or in combination with non-renewable sources) and the different techniques used for the manufacture of such films. However, no previous work was found in the specialized literature on the production of edible biodegradable films based on quinoa starch using the wet method. Thus the aim of this work was to develop biodegradable films based on quinoa starch, and evaluate the combined effects of the glycerol content (16.6; 20; 25; 30; 33.4), pH (9.7; 10; 10.5; 11; 11.3) and drying conditions (30 °C/20 h; 34 °C/17 h; 40 °C/10 h; 46 °C/9 h; 50 °C/5 h;) on the mechanical properties and water solubility of the films using response surface methodology (RSM). The equations resulting from the RSM analysis were used to optimize the quinoa starch film (QSF) formulations, and finally the optimized QSF was characterized with respect to its mechanical, optical, solubility and barrier properties.

## 2. Materials and methods

### 2.1. Quinoa seeds

Polished mature seeds of quinoa (*C. quinoa*, Willdenow) cultivar “Real” were purchased in Municipal Market of Ayacucho – Perú. The seeds were cleaned up and stored at 3 °C in sealed containers until they were tested. Glycerol, NaOH, KOH and HCl were analytical reagent grade and were purchased from Merck (São Paulo, Brazil).

### 2.2. Quinoa starch production

Quinoa starch was produced using the methodology involving a short contact time with dilute alkaline solutions developed by Araujo-Farro (2008). The grains (1 kg) were first washed at least four times in an excess of deionized water in order to remove the saponins that cover the quinoa seeds and which are totally soluble in water. The seeds were then steeped in deionized water at 3 °C (1 kg seed/2 kg deionized water) for 8 h. The softened grain suspension was then milled in a kitchen blender and the resulting slurry screened and washed through a series of sieves (80, 200 and 270 mesh) with deionized water. The sieving-washing procedure was repeated five times until there was no further starch-like color associated with the material retained on the sieves. The spent material retained on the sieves then being discarded. The material that passed through the sieves was centrifuged (600 g, 20 min, 4 °C), and the upper layer containing the protein and fine fiber found on top of the sediment, was removed. The remaining starch cake was resuspended in deionized water, centrifuged, and the dark upper layer removed, repeating this process five times in all. The starch collected at the end of this process was suspended in aqueous 0.20% (w/w) NaOH at an alkaline pH value of 10.5, and gently stirred for 5 min at 15 °C to avoid any rise in temperature during this process. The suspension was then centrifuged, resuspended in deionized water and neutralized carefully by adding 1 M HCl. After centrifugation, the starch cake was resuspended in deionized water, centrifuged and removed (five times) in order to remove any traces of the mucilaginous layer (residual protein material) in the upper layer and any ionic components of the NaCl resulting from the neutralization process. The purified starch was then frozen in liquid nitrogen and freeze dried (HETO, CT 60E, Denmark), which took a week. The dried starch was gently ground by hand with a pestle and mortar and passed through a 270 mesh sieve. The obtained quinoa starch was stored at 3 °C in sealed containers until it was used.

#### 2.2.1. Proximate analysis

The content of protein, ash, ether extractable lipids, total fiber and water was analyzed following the standard methods of the AOAC (1995).

Amylose content was determined using a colorimetric method (Juliano, 1971) modified by Martinez and Cuevas (1989).

### 2.3. Preparation of quinoa films and sample conditioning for the mechanical and solubility tests

All film-forming solutions (FFS) composed of quinoa (*C. quinoa*, Willdenow) starch were prepared, according to the experimental design shown in Table 1. The quinoa starch content, glycerol concentration, pH values, drying conditions and quinoa film-technique were established according to preliminary tests (Araujo-Farro, 2008). To obtain quinoa starch FFS, starch quinoa powder (4 g/100 g total film solution) was dispersed in deionized water (18 meq) at room temperature and stirred for at least 1 h on a magnetic stirrer (TECNAL-TE085). The pH value was then adjusted to the alkaline values shown in Table 1 using a 1N NaOH solution, in order to dissolve the protein and facilitate starch granule disruption during the gelatinization process. After adjusting the pH, magnetic stirring was continued for at least one more hour, and the dispersion then heated to 50 °C, and maintained at this temperature for a further 45 min, with gentle magnetic stirring. The quinoa starch dispersion was gelatinized at 97 °C for 30 min with constant stirring in a water bath (TECNAL, TE184, Brazil). The glycerol was then added and stirring continued for another 15 min in order to completely homogenize the FFS. The FFS was then poured evenly onto polycarbonate plates (≈12 × 12 cm), and the weight controlled (±0.001) using a semi-analytical balance (SCIENTECH, model AS 210, 210 g, ±0.0001 g) so as to obtain a constant film thickness of 80 ± 2 μm. The films were dehydrated in an oven with air renewal and circulation and controlled temperature and relative humidity (MARCONI, model MA037, São Paulo, Brazil), using the different drying conditions determined by the experimental design (Table 1) and 55% relative humidity (RH). The dried quinoa starch films (QSF) were peeled off the casting surface, cut into adequate samples and conditioned at 25 °C and 58% RH in desiccators with saturated solutions of NaBr for 72 h prior to characterization. The thickness of the conditioned films was measured with a digital micrometer (±0.001 mm, probe diameter of 6.4 mm, Mitutoyo, Suzano, Brazil), and the value reported was the average of 15 measurements made at ten different locations. All the tests were carried out in air-conditioned rooms (T = 25 °C and relative humidity between 55 and 65 °C).

### 2.4. Experimental design

A 2<sup>3</sup> full-factorial central composite design (star configuration) with 6 axial and 3 central points, resulting in 17 experiments, was used to obtain a second-order model for prediction of mechanical properties such as tensile strength ( $Y_1$ ), elongation at break ( $Y_2$ ), Young's modulus ( $Y_3$ ), puncture force ( $Y_4$ ), puncture deformation ( $Y_5$ ), as well as solubility ( $Y_6$ ), which were denoted as dependent variables, as a function of three variables (independent variables): glycerol content ( $X_1$ ), pH levels ( $X_2$ ) and drying conditions ( $X_3$ ). The dependent variables were expressed individually as a function of the aforementioned independent variables using the following polynomial equation (1):

$$Y = \beta_0 + \beta_1 X_1 + \beta_2 X_2 + \beta_3 X_3 + \beta_{11} X_1^2 + \beta_{22} X_2^2 + \beta_{33} X_3^2 + \beta_{12} X_1 X_2 + \beta_{13} X_1 X_3 + \beta_{23} X_2 X_3 \quad (1)$$

The statistical design and the coded and real values of these variables are given in Table 1. All experiments were performed randomly, and data were treated with the aid of STATISTICA 5.0 from Statsoft Inc (Colla et al., 2006; Khuri & Cornell, 1996).

**Table 1**  
Experimental design for the quinoa starch (QSF) films tests and data values of tensile strength (TS), elongation at break (ELOB), Young's modulus (YM), puncture force (PF), puncture deformation (PD) and solubility (S) for the 17 trials of the QSF.

Tests	Independents factors			Dependent factors					Solubility (% d.b.)
	Glycerol content (GC)	pH	Drying conditions (DC) (°C/h)	Tensile test					
				Tensile strength (TS) (MPa)	Elongation at break (ELOB) (%)	Young's modulus (YM)	Puncture force (PF) (N)	Puncture deformation (PD) (%)	
1	20 (−1)	10 (−1)	34/17 (−1)	17.88	3.39	10.87	6.88	0.90	15.9
2	30 (+1)	10 (−1)	34/17 (−1)	3.18	101.01	0.45	4.29	8.34	18.3
3	20 (−1)	11 (+1)	34/17 (−1)	15.87	4.54	8.68	6.30	0.81	15.5
4	30 (+1)	11 (+1)	34/17 (−1)	3.39	96.65	0.60	4.81	6.72	20.2
5	20 (−1)	10 (−1)	46/9 (+1)	17.48	2.45	9.52	7.22	0.86	17.6
6	30 (+1)	10 (−1)	46/9 (+1)	3.14	92.79	0.42	4.20	8.92	21.1
7	20 (−1)	11 (+1)	46/9 (+1)	13.29	3.30	8.49	6.68	1.13	17.7
8	30 (+1)	11 (+1)	46/9 (+1)	3.82	90.19	0.64	4.63	10.84	22.3
9	16.6 (−1.681)	10.5 (0)	40/10 (0)	23.90	2.10	13.74	7.99	0.59	14.4
10	33.4 (+1.681)	10.5 (0)	40/10 (0)	2.63	118.10	0.28	3.50	10.93	23.3
11	25 (0)	9.7 (−1.681)	40/10 (0)	5.30	69.79	2.89	5.59	3.91	19.9
12	25 (0)	11.3 (+1.681)	40/10 (0)	6.07	63.02	3.59	6.49	4.11	18.6
13	25 (0)	10.5 (0)	30/20 (−1.681)	6.00	78.75	2.84	6.25	4.01	18.4
14	25 (0)	10.5 (0)	50/5 (+1.681)	6.92	35.79	4.52	7.30	3.30	19.2
15	25 (0)	10.5 (0)	40/10 (0)	4.64	82.10	1.73	6.10	5.45	17.0
16	25 (0)	10.5 (0)	40/10 (0)	5.14	88.25	1.91	6.20	5.95	16.1
17	25 (0)	10.5 (0)	40/10 (0)	4.91	85.12	1.82	6.40	5.72	16.9

Glycerol content = GC = (g glycerol/100 g of starch d.b.).

## 2.5. Characterization of quinoa starch films

Quinoa starch films were characterized by determinations of mechanical properties and solubility. The QFS obtained under optimized conditions (glycerol content (GC), alkaline pH value and drying condition (DC)) were also analyzed by mechanical properties, solubility, optical properties (color, opacity), oxygen permeability, water vapor permeability and scanning electron microscopy (SEM).

### 2.5.1. Mechanical properties

Mechanical properties were determined by the tensile test (tensile strength, TS, and elongation at break, ELOB) and puncture test (puncture force, PF, and puncture deformation, PD) using a TA-XT2i Stable Micro Systems texture analyzer (SMS). The tensile test was performed according to the ASTM standard method D882-97 (ASTM, 1997). Quinoa starch films samples were cut for each film with 100 mm in length and 16 mm in width at the middle. The initial grip separation was set at 80 mm and the crosshead speed at 1.0 mm/s. At least five samples from each film were evaluated. The tensile strength (force/initial cross-sectional area) and elongation at break ( $\Delta l/l_0$ ) were determined with the software Texture Expert V.1.15 (SMS) directly from the stress x strain curves. Elongation at break was obtained using Eq. (2):

$$\text{ELO} = 100 \left( \frac{\Delta l}{l_0} \right) \quad (2)$$

where  $\Delta l$  is the elongated distance at break and  $l_0$  the initial distance between the grips (80 mm).

For the puncture test, circular sample films were fixed in a 40 mm diameter cell and perforated using a 3 mm diameter cylindrical probe moving at 1 mm/s (Gontard, Guilbert, & Cuq, 1993), in triplicate. The puncture force was determined with the software Texture Expert V.1.15 (SMS) directly from the force displacement curves. The puncture deformation was calculated using Eq. (3):

$$\text{PD} = \frac{\Delta l}{l_0} = \frac{\left[ \sqrt{(D^2 + l_0^2)} - l_0 \right]}{l_0} \quad (3)$$

where  $l_0$  is the initial disc radius (17 mm) and  $D$  the distance penetrated at the break point.

### 2.5.2. Solubility in water

The solubility was calculated as the percentage of dry matter of the film solubilized after immersion for 24 h in water at 25 °C (Colla et al., 2006; Gontard, Duchez, Cuq, & Guilbert, 1994). Discs of film (2 cm diameter) were cut, weighed, immersed in 50 mL of distilled water, and slowly and periodically agitated. The amount of dry matter of initial and final samples was determined by drying the samples at 105 °C for 24 h. The solubility was calculated using Eq. (4):

$$S = 100 \left[ \frac{w_i - w_f}{w_i} \right] \quad (4)$$

where  $S$  = solubility;  $w_i$  and  $w_f$  were the initial and final weight of the disc on dry basis, respectively.

### 2.5.3. Water vapor permeability

Water vapor permeability (WVP) tests were conducted using ASTM standard method E96-95, (ASTM, 1995), considering the modifications proposed by Gontard et al. (1993). Each film sample was sealed over the circular opening of a permeation cell containing silica gel. These cells were placed on desiccators with distilled water kept at 25 °C. After the samples had reached steady-state conditions (~20 h), the cell weight was measured each 24 h, for 9

days, using an analytical balance (OHAUS, model Analytical Plus 200g,  $\pm 0.00001$  g). The WVP was calculated as Eq. (5):

$$\text{WVP} = \left( \frac{w}{t} \right) \times \frac{1}{A} \times \frac{x}{\Delta P} \quad (5)$$

where  $x$  is the average thickness of the quinoa starch films,  $A$  is the permeation area ( $0.00091 \text{ m}^2$ ),  $\Delta P$  is the difference between the partial pressure of the atmosphere over silica gel and over pure water ( $3.168 \text{ kPa}$ , at  $25^\circ\text{C}$ ) ( $2.642 \text{ Pa}$ , at  $22^\circ$ ), and the term  $(w/t)$  was calculated by linear regression using data of weight gain as a function of time. All tests were performed in triplicate.

#### 2.5.4. Oxygen permeability

Oxygen permeability measurements were performed on a Mocon Ox-Tran 2/20 instrument equipped with a Coulox sensor (Modern Control, Inc., Minneapolis, MN) operating according to ASTM standard method D3985-81 (ASTM, 1989) (Colla et al., 2006) at atmospheric pressure and room temperature ( $25^\circ\text{C}$ ). The test cell was composed of two chambers separated by the films ( $5 \text{ cm}^2$ ), one of them containing 100% oxygen and the other one containing nitrogen, which induced the transfer of oxygen through the film to the coulometric sensor. The measurements were taken at  $25^\circ\text{C}$ , when oxygen flux had already stabilized, indicating that steady state was reached. The oxygen permeability (OP) was calculated by dividing the oxygen transmission rate by the oxygen pressure and multiplying this result by the mean thickness of the sample.

#### 2.5.5. Film color

The color of the quinoa starch samples was determined with a colorimeter (Hunter Lab system, model Miniscan XE, USA), operating with  $D_{65}$  (day light) and a measuring cell with an opening of  $30 \text{ mm}$ , using the CIELab color parameters (Gennadios, Weller, Hanna, & Froning, 1996). The color and the CIELab color difference meter identifies color in three attributes,  $L^*$  (white = 100; black = 0),  $a^*$  (positive = red; negative = green), and  $b^*$  (positive = yellow; negative = blue). The instrument was calibrated using a white standard color calibration plate. The color difference ( $\Delta E^*$ ), compared to a white standard tile having colorimeter color values of  $L_s^* = 94.71$ ;  $a_s^* = -0.76$  and  $b_s^* = 1.55$ , was calculated using the Eq. (6)

$$\Delta E^* = \sqrt{(L^* - L_s^*)^2 + (a^* - a_s^*)^2 + (b^* - b_s^*)^2} \quad (6)$$

where  $L^*$ ,  $a^*$  and  $b^*$  are the color attribute of the quinoa starch film samples and  $L_s^*$ ,  $a_s^*$  and  $b_s^*$  are the color parameter of the white standard tile.

**Table 2**  
Results for regression coefficients and analysis of variance (ANOVA) for puncture force (PF), puncture deformation (PD), tensile strength (TS), elongation at break (EB), elastic modulus (EM), water solubility (S), puncture force (PF) and puncture deformation (PD).

Coefficients				TS (MPa) $Y_1$	ELOB (%) $Y_2$	YM (MPa/%) $Y_3$	PF (MPa) $Y_4$	PD (%) $Y_5$	S (%) $Y_6$
Independent				$\beta_0$	4.85	85.85	1.81	6.54	16.70
Linear	Glycerol	$X_1$	$\beta_1$	−6.36	41.18	−4.25	−1.22	3.55	2.20
	pH	$X_2$	$\beta_2$	−0.29	−	−0.12	−	−	−
	DC	$X_3$	$\beta_3$	−	−6.53	0.09	0.16	0.28	0.74
Quadratic	Glycerol	$X_1^2$	$\beta_1^2$	3.20	−11.21	1.87	0.32	−	0.66
	Ph	$X_2^2$	$\beta_2^2$	0.52	−8.98	0.53	−0.21	−0.54	0.79
	DC	$X_3^2$	$\beta_3^2$	0.79	−12.22	0.69	−	−0.67	0.63
Interactions	Gly $\times$ pH	$X_{12}$	$\beta_{12}$	0.89	−	0.45	−	−	−
	Gly $\times$ DC	$X_{13}$	$\beta_{13}$	0.42	−	0.19	−	0.55	−
	pH $\times$ DC	$X_{23}$	$\beta_{23}$	−	−	0.16	−	0.49	−
$F_{\text{Calculate}}$				98.56	47.13	64.67	25.59	46.67	18.8
$F_{\text{Listed}}$				3.29	3.68	3.68	2.45	2.46	3.22
$F_{\text{Calculate}}:F_{\text{Listed}}$				29.95	12.81	17.57	10.44	18.97	5.83
$p <$				0.05	0.05	0.10	0.10	0.10	0.05

TS: tensile strength; ELOB: elongation at break; YM: Young's modulus; PF: puncture force; PD: puncture deformation; S: solubility.

#### 2.5.6. Film opacity

Film opacity was determined according to the Hunterlab method in the reflectance mode (Gontard et al., 1993). Opacity ( $Y$ ) was calculated from the relationship between the opacity of the film superposed on the black standard ( $Y_{\text{black}}$ ) and that of the film superposed on the white standard ( $Y_{\text{white}}$ ) according to the following equation (7):

$$Y = \frac{Y_{\text{black}}}{Y_{\text{white}}} \times 100 \quad (7)$$

#### 2.5.7. Scanning electron microscopy (SEM)

SEM analyses were performed using a scanning electron microscope (SEM) (MEV JEOL/JSM-5800LV/Scanning Microscope-UK). The optimized quinoa starch films (QSFOPT) samples were maintained in a desiccator with silicagel for 2 weeks and then mounted on an aluminum stub using a double-sided copper tape. Further, the stubs with QSF samples were coated with gold in a sputter coater (Sputter Coater Balzers-model SCD 050) for 240 s at 40 mA. The QSFOPT samples were viewed with SEM operating at 10 kV (Colla et al., 2006).

### 3. Results

#### 3.1. Proximate composition of the quinoa starch

The Araujo-Farro (2008) method of quinoa starch extraction developed on a laboratory scale, produced a material containing, on dry weight basis,  $0.9 \pm 0.02\%$  total protein,  $0.01 \pm 0.001\%$  ether extractable lipids,  $0.23 \pm 0.02\%$  total fiber,  $0.21 \pm 0.06\%$  total ash,  $17.1 \pm 0.05\%$  amylase.

#### 3.2. Quinoa starch films

All the quinoa starch films (QSF) prepared according to the experimental design were self-supporting, peelable, colorless, transparent, flexible, easily handled and with a homogeneous, smooth surface. The average thickness of the films was  $0.80 \pm 0.002 \text{ mm}$ . In order to obtain constant thickness of the QSF, with low standard deviation of the means, a strict control of the ratio between the amount of dry mass of the film-forming solution and the casting support area was required, a procedure consistent with that used in other research studies on films (Colla et al., 2006; Mali et al., 2002; Mali, Grossmann, et al., 2005). After the conditioning time the films were characterized, obtaining the

experimental data for puncture deformation (PD), puncture force at break (PF), tensile strength (TS), elongation at break (ELOB), Young's modulus (YM) and solubility (S), as shown in Table 1 for the films prepared according to the previously described experimental design. These data were submitted to statistical analyses, including fitting to Eq. (1), followed by an analysis of variance (ANOVA) at the 95% and 90% confidence levels, and only the statistically significant parameters were used to analyze the behavior of the fitted mathematical models. The resulting equations were tested for their adequacy and fitness by ANOVA with the aid of STATISTICA version 5.0. Table 2 shows the results of the ANOVA, including the regression coefficients for the coded second-order polynomial equation, the determination coefficients ( $R^2$ ) and the  $F$  and  $p$  values. Finally, to determine if the fitted equations (FE) were predictive so as to plot the response surfaces, the FE must satisfy a certain criterion based on the  $F_{\text{test}}$  values ( $F_{\text{calculated}}$  and  $F_{\text{listed}}$ ) and consequently on

the calculated  $F$  ratio value, for the regressions related to the residuals ( $F_{\text{cal}}:F_{\text{list}}$ ). The value of this ratio must be higher than that of  $F_{\text{list}}$  (Khuri & Cornell, 1996). According to this criterion, every fitted equation for each dependent variable established in this study was predictive, since all of them presented  $F$  ratio values three times higher than the corresponding  $F$  listed value. All the results suggested that the fitted models were suitable (significant and predictive), showing significant regression, low residual values, no lack of fit and satisfactory determination coefficients.

### 3.2.1. Mechanical properties according to tensile tests

3.2.1.1. Tensile strength (TS). According to the results of ANOVA (Table 2), the calculated coded mathematical model for tensile strength (TS), represented by Eq. (8), was statistically significant ( $p < 0.05$ ;  $R_2 = 0.999$ ) and predictive ( $F_{\text{Calc}} = 29.9F_{\text{List}}$ ), allowing for

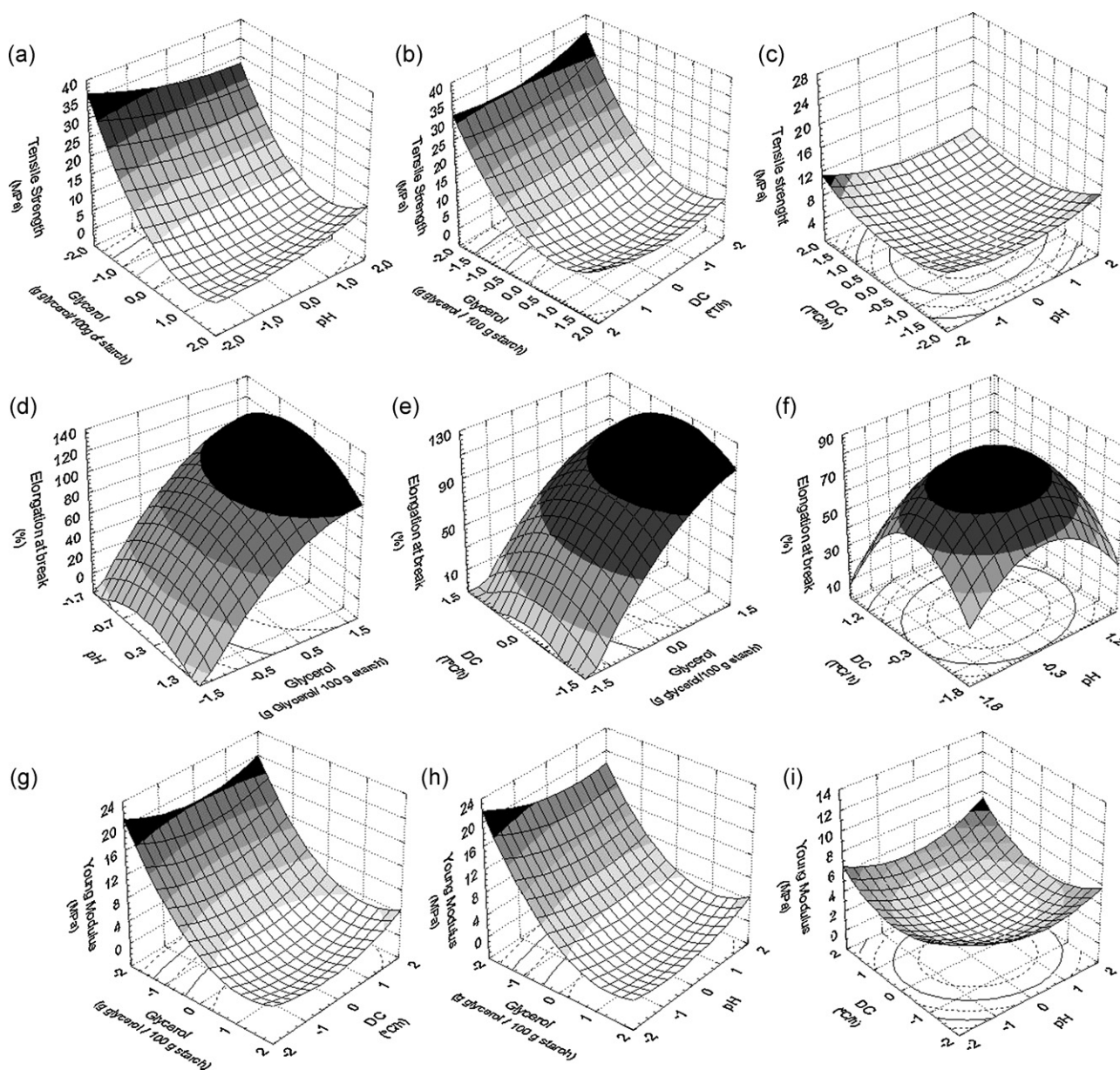


**Fig. 1.** Response surfaces for tensile strength (MPa) as a function of (a) pH and glycerol concentrations (g/100 g of starch), (b) drying conditions (DC;  $T^{\circ}\text{C/h}$ ) and glycerol concentrations (g/100 g of starch), (c) pH and drying conditions (DC;  $T^{\circ}\text{C/h}$ ); response surfaces elongation at break (%) as a function of (d) glycerol concentrations (g/100 g of starch) and pH, (e) glycerol concentrations (g/100 g of starch) and drying conditions (DC;  $T^{\circ}\text{C/h}$ ), (f) pH and drying conditions (DC;  $T^{\circ}\text{C/h}$ ); response surfaces for Young's modulus (MPa) as a function of (g) drying conditions (DC;  $T^{\circ}\text{C/h}$ ) and glycerol concentrations (g/100 g of starch), (h) pH and glycerol concentrations (g/100 g of starch), (i) pH and drying conditions (DC;  $T^{\circ}\text{C/h}$ ).

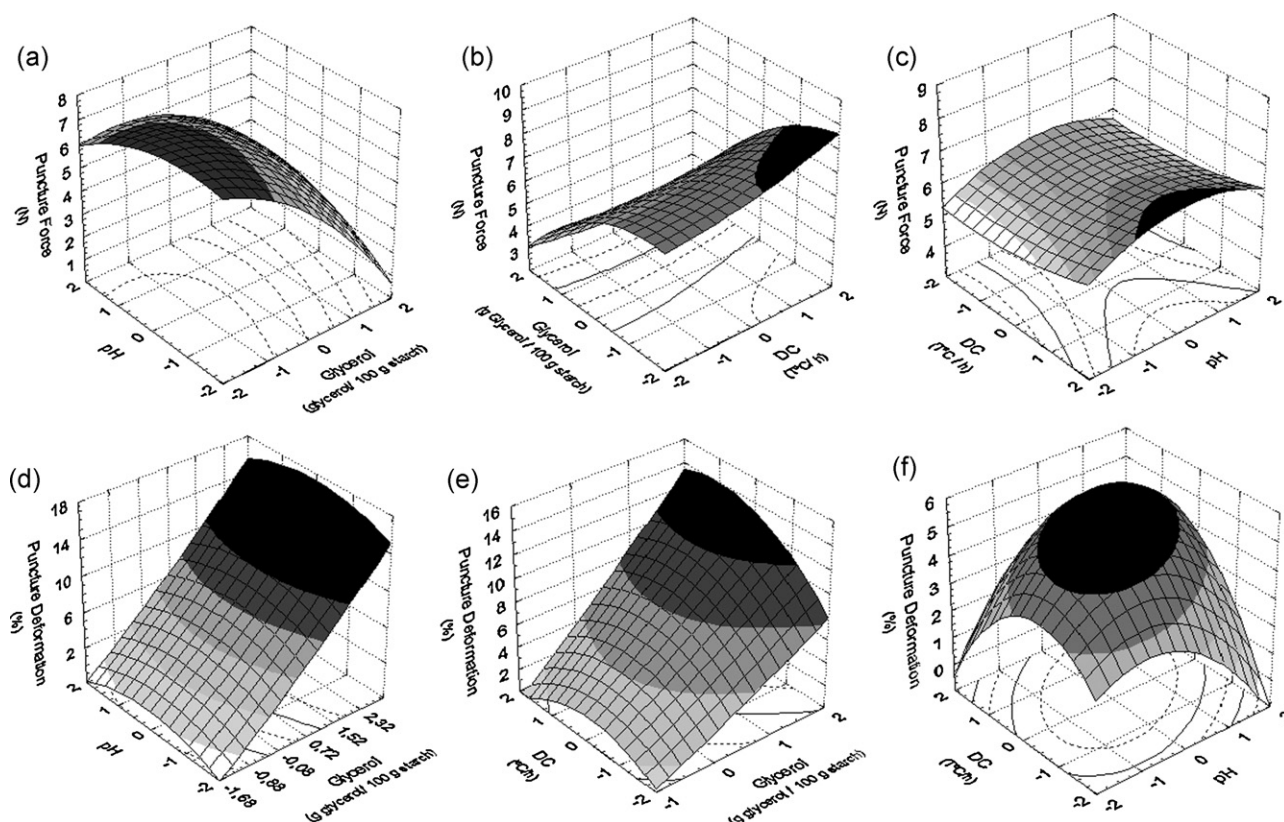


**Fig. 2.** Response surfaces for puncture force (N) as a function of (a) glycerol concentrations (g/100 g of starch) and pH, (b) drying conditions (DC; T°C/h) and glycerol concentrations (g/100 g of starch), (c) pH and drying conditions (DC; T°C/h). Response surfaces for puncture deformation (%) as a function of (d) glycerol concentrations (g/100 g of starch) and pH, (e) glycerol concentrations (g/100 g of starch) and drying conditions (DC; T°C/h) and (f) pH and drying conditions (DC; T°C/h).

plotting of the response surfaces (Fig. 1a–c).

$$Y_1 = TS = 4.85 - 6.36X_1 - 0.29X_2 + 3.20X_1^2 + 0.52X_2^2 + 0.79X_3^2 + 0.89X_1X_2 + 0.42X_1X_3 \quad (8)$$

According to Eq. (8), the most relevant variable with respect to TS, was the glycerol concentration (GC;  $X_1$ ), including its interactions with the pH ( $X_2$ ) value and the drying conditions (DC;  $X_3$ ), followed by the pH value with a smaller contribution, whereas the DC term did not directly affect TS as a linear component, only by its interaction with glycerol.

**3.2.1.2. Elongation at break (ELOB).** The ANOVA for the coded mathematical model for ELOB indicated that the model was statistically significant ( $p < 0.05$ ;  $R^2 = 0.96$ ) and predictive with  $F_{\text{Calc}} = 12.8F_{\text{List}}$ . The coded second-order model (Eq. (9)) for this variable was as follows:

$$Y_2 = \text{ELOB} = 85.85 + 41.18X_1 - 6.53X_3 - 11.21X_{12} - 8.98X_2^2 - 12.22X_3^2 \quad (9)$$

According to Eq. (9), ELOB was significantly affected by the GC ( $X_1$ ;  $p < 0.05$ ) and DC, while the alkali pH value ( $X_2$ ) affected it by

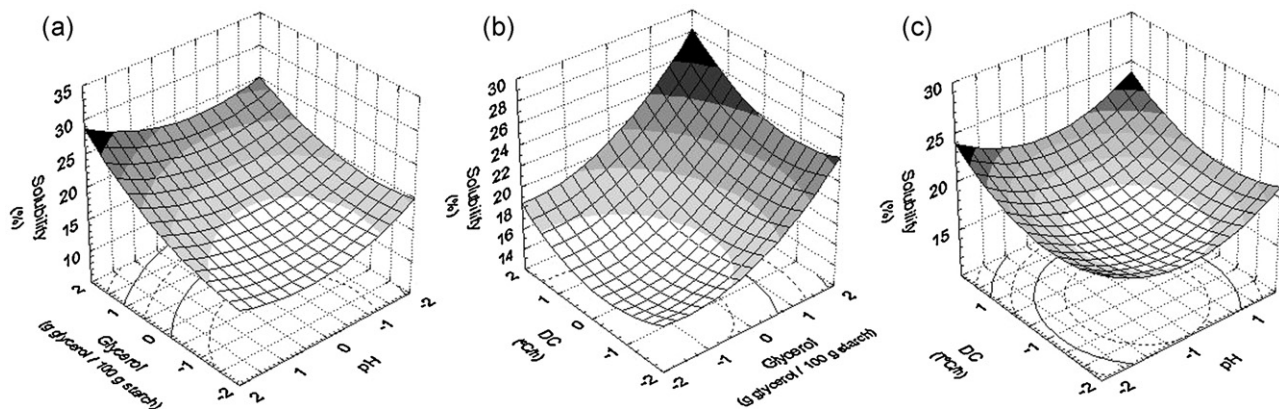


**Fig. 3.** Response surfaces for solubility (%) as a function of (a) pH and glycerol concentrations (g/100 g of starch), (b) glycerol concentrations (g/100 g of starch) and drying conditions (DC; T°C/h), (c) pH and drying conditions (DC; T°C/h).

means of the interaction terms ( $X_{12}$ ; GC and pH), and quadratic term ( $X_2^2$ ). Eq. (9) was used to plot the ELOB response surfaces presented in Fig. 1(d–f).

**3.2.1.3. Young's modulus (YM).** Young's modulus or the elastic modulus is the fundamental measurement for film stiffness, such that the higher the YM, the stiffer the material (Mali, Grossmann, et al., 2005; Mali, Sakanaka, et al., 2005). For the YM, all the effects and interactions were statistically significant ( $p < 0.05$ ;  $R^2 = 0.96$ ) and predictive ( $F_{\text{Calc}} = 17.6F_{\text{List}}$ ) and the followed coded model (Eq. (10)) was obtained

$$Y_3 = \text{YM} = 1.81 - 4.25X_1 - 0.12X_2 + 0.09X_3 + 1.87X_1^2 + 0.53X_2^2 + 0.69X_3^2 + 0.45X_1X_2 + 0.19X_1X_3 + 0.16X_2X_3 \quad (10)$$

The YM was more significantly affected by the GC ( $p < 0.10$ ). The alkaline pH values and DC showed weaker, but nevertheless statistically significant influences. Eq. (10) was used to plot the YM response surfaces presented in Fig. 1(g–i).

### 3.2.2. Mechanical properties according to puncture tests

**3.2.2.1. Puncture force at break (PF).** Based on the regression analysis and ANOVA results (Table 2), the second-order mathematical model was statistically significant and predictive for PF (Eq. (4);  $p > 0.10$ ;  $R^2 = 0.92$ ;  $F_{\text{Calc}} = 10.4F_{\text{List}}$ ) and for puncture deformation (Eq. (11);  $p > 0.10$ ;  $R^2 = 0.92$ ;  $F_{\text{Calc}} = 18.97F_{\text{List}}$ ).

$$Y_4 = \text{PF} = 6.54 - 1.22X_1 + 0.16X_3 + 0.32X_1^2 - 0.21X_2^2 \quad (11)$$

**3.2.2.2. Puncture deformation (PD).** The fitted PD equation (Eq. (12)) was more significantly affected by the GC ( $X_1$ ;  $p < 0.05$ ), followed by a weaker influence of the DC ( $X_3$ ) and the interaction between this variable with GC and the pH value ( $X_2$ ). The pH value did not directly affect it as a linear component, only by quadratic term ( $X_2^2$ ) and the interaction of the means with the DC ( $X_2X_3$ ).

$$Y_5 = \text{PD} = 5.28 + 3.55X_1 + 0.28X_3 - 0.54X_2^2 - 0.67X_3^2 + 0.55X_1X_3 + 0.49X_2X_3 \quad (12)$$

The response surfaces plotted using Eqs. (11) and (12) are shown in Fig. 2(a–c) and (d–f), respectively. The puncture test results verified the same trend as the tensile tests, a high influence of GC ( $X_1$ ) on the response variables, with the alkaline pH values ( $X_2$ ) and DC ( $X_3$ ) showing smaller contributions.

### 3.2.3. Solubility in water

As for the tensile and puncture tests, a regression analysis was also performed to obtain a second-order model equation (Eq. (13)) for solubility as a function of the GC ( $X_1$ ), alkaline pH value ( $X_2$ ) and DC ( $X_3$ ).

$$Y_6 = S = 16.70 + 2.20X_1 + 0.74X_3 + 0.66X_1^2 + 0.79X_2^2 + 0.63X_3^2 \quad (13)$$

From the ANOVA (Table 2), the resulting second-order model fitted for the solubility property was also statistically significant ( $p < 0.05$ ;  $R^2 = 0.90$ ) and predictive ( $F_{\text{Calc}} = 5.83F_{\text{List}}$ ). According to this equation, the GC and DC affected solubility positively and linearly, while the pH value affected as a quadratic term. Equation (13) was used to plot the solubility response surface presented in Fig. 3(a–c).

## 4. Discussion

As can be seen from Table 1, the QSF elaborated according to run 9, with a glycerol concentration (GC) of 16.6%, an alkaline pH value

of 10.5 and drying conditions (DC) of 40 °C/10 h, showed the highest TS (23.90 MPa), YM (13.74 MPa/%) and PF (7.99 N) values, whereas ELOB and PD showed the lowest values of 2.10% and 0.59%, respectively. On the other hand, the QSF elaborated according to run 10, with a glycerol concentration of 33.4%, alkaline pH value of 10.5 and drying conditions of 40 °C/10 h, showed the highest values for ELOB (118.10%) and PD (10.93%). However, under these conditions the lowest values for TS (2.63 MPa), YM (0.28 MPa/%) and PF (3.50 N) were observed. Therefore it can be seen that the addition of glycerol greatly (30–34%) increased quinoa starch film (QSF) flexibility and extensibility, at the same time reducing material resistance (TS and PF). This behavior can be more effectively explained and observed from the analysis of the variables in the fitted equations (Eqs. (8)–(12)) and their respective response surfaces (Figs. 1 and 2) for the mechanical properties, obtained from the statistical analysis shown in Table 2. The value for GC had a negative effect on TS, YM and PF but a positive effect on ELOB and PD. This behavior of the GC is in agreement with other studies, and can be explained by the plasticizing effect of glycerol (Vanin, Sobral, Menegalli, Carvalho, & Habitante, 2005; Mali, Sakanaka, et al., 2005). The major positive effect of the glycerol concentration on ELOB can be explained by its plasticizing effect on the QSF structure (Eq. (9), Fig. 1d and e). According to Mali et al. (2002) and Mali, Grossmann, et al. (2005) and Mali, Sakanaka, et al. (2005), films with glycerol added as a plasticizer, weaken and decrease the intermolecular forces or attractive forces between the adjacent polymer chains, reducing the glass transition temperature ( $T_g$ ) of starch-based materials. In addition, as explained by Myllärinen, Partanen, Seppälä, and Forsell (2002) in their study on the influence of glycerol on edible amylose and amylopectin films, the amylose/amylopectin ratio, plasticizer used and/or the water content and storage conditions, can affect the mechanical properties of starch films due to their effect on the  $T_g$ . As expected, the response surface plots (Fig. 1a and b) show that the GC had a strong, negative effect on the TS (Table 2), since this plasticizer is hygroscopic and increases the mobility of the molecules throughout the film structure (Colla et al., 2006; Mali et al., 2002), and it is possible that this increase in molecular mobility caused the increase in ELOB and hence the reduction in TS, both strongly influencing the QSF. The alkaline pH values did not have a remarkable effect on the tensile strength properties, but, on the other hand, this parameter showed an interesting negative effect on TS (Fig. 1a and c), that is, an increase in this parameter also resulted in lower TS values. The ANOVA (Table 2) confirmed that the DC had a significant, negative but relevant effect on the ELOB (Table 2, Eq. (9), Fig. 1e and f), more than on the fitted equations for the other mechanical properties. According to Table 1, the results for runs 13 and 14, where both the GC and alkaline pH value were fixed (25% and 10.5, respectively), while the DC of these runs were fixed at the extreme values, represented by the axial coded levels (run 13; −1.68; 30 °C/20 h and run 14; +1.68; 50 °C/5 h), showed that increasing the temperature of the film drying conditions formed films with decreased ELOB. On the other hand, high values for elongation at break corresponded to the central point values for the temperature of the drying conditions and pH (Fig. 1d–f). From the present results, it could be hypothesized that this central value of drying conditions (40 °C/10 h) of the QSF allowed for better amylose–amylopectin–glycerol–water/biopolymer arrangement and cohesion within the QSF matrix, resulting in a elastic, more compact structure (Fig. 4).

According to the response surfaces, Fig. 3(a–c), the minimum value for solubility was a function of the independent variables (16.6–22% glycerol, pH values from 10 to 11 and drying conditions between 40 °C/10 h and 30 °C/20 h). The values for solubility, as observed in Table 1, ranged from 14.4 to 23.3%. These very low values obtained from the QSF were a consequence of the high level of cohesion within the QSF matrix, resulting in a compact structure.

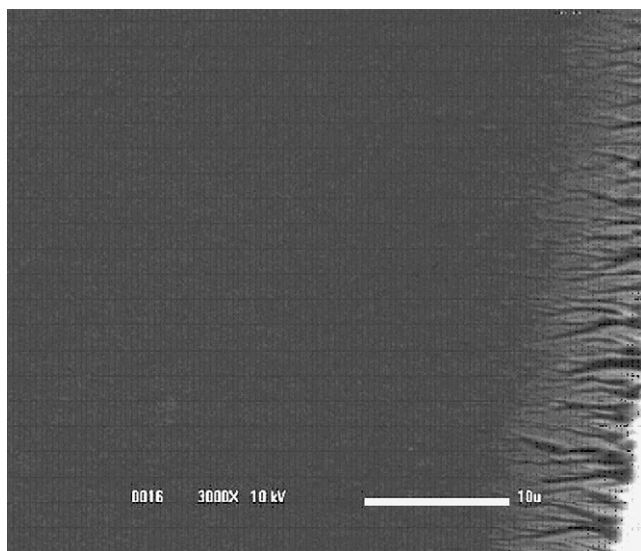


**Fig. 4.** Scanning electron microscopy (SEM) of optimized quinoa starch films (QSFOPT; GC = 21.2 g of glycerol/100 g of starch; alkaline pH value of 10.7; and drying conditions of 36 °C/14 h).

This specific QSF matrix structure is related to the specific proximate composition of the quinoa starch, and also to the film-forming technique used in this study, more specifically to the gelatinization process, which was carried out in an alkaline medium. According to Rooney and Suhendro (1999), the alkaline-thermal treatment is used to promote total disruption of the starch granules, allowing for total leaching of the amylose and swelling of the amylopectin during the starch gelatinization process, and also to dissolve some of the proteins surrounding the starch granule. This would help improve the physical properties of the QSF, since the quinoa starch had an amylose content of 17.1% and amylopectin content of 89.9%, leading to the formation of cohesive, more structured films. In addition, according to their study on the influence of glycerol on edible amylose and amylopectin films, Myllärinen et al. (2002) concluded that amylose films exhibited better mechanical properties than amylopectin films.

## 5. Properties of the quinoa starch films prepared using the best formulation (QSFOPT)

Since the main mechanical characteristics of flexible packaging are resistance and, obviously, flexibility, the tensile strength and elongation at break together with solubility, were the properties considered to determine the optimal conditions in the response surface analysis. A common optimum value for the three response variables (TS, ELOB, S) was obtained utilizing desirability method, the results obtained suggested the following as the best or optimal formulation: 4% quinoa starch, 21.2% glycerol, a pH value of 10.7 and drying conditions of 36 °C/14 h. Table 3 shows the properties of the films prepared using those optimal formulation. The tensile stress (7.56 MPa) of the QSFOPT was similar to that obtained for the 70 μm thick yam starch film (7.84 MPa) and higher than that of the 110 μm thick yam starch film (4.70 MPa). With respect to the value obtained for ELOB (58.14%), this value was higher than those obtained for both yam starch films. The low value obtained for solubility (15.20%) for this optimized formulation was related to the dense starch biopolymer-protein matrix and probably also to interactions between inter-granular lipids and the amylose and amylopectin starch biopolymers (Araujo-Farro, 2008; Van Soest, Hulleman, Wit, & Vliegenthart, 1996). These interactions formed the amylose-lipid (AL) and amylopectin-lipid (AML) complexes, which resulted from the alkaline-thermal treatment and later became well defined or well structured during the low temperature drying conditions applied in this study. According to Rooney and Suhendro (1999), the alkaline-thermal treatment has several functions, such as facilitating and decreasing the granule starch disruption time, dissolving the protein, saponifying part of the inter-granular lipids and consequently leading to the formation of hydrophobic AL and AML. These AL and AML probably conferred special hydrophobic properties on the QSF, as reflected in the low values for solubility shown throughout the results of the experimental design (in the present study). The barrier properties (water vapor and oxygen permeability) presented by the optimized QSF formulation were ( $WVP = 5.6 \times 10^{-11} \text{ g m}^{-1} \text{ s}^{-1} \text{ Pa}^{-1}$ ;  $O_2 P = 0.50 \times 10^{-13}$ ), respectively. The value for WVP was lower than the values presented by Tapia-Blácido, Sobral, and Menegalli (2005) and Colla et al. (2006), working with amaranth films plasticized with glycerol and with stearic acid and glycerol, respectively (Table 4). The QSF produced under the optimized conditions exhib-

**Table 3**  
Properties of quinoa (*Chenopodium quinoa* Willdenow) starch film made with the optimized formulation.

Properties	Value
Thickness	$0.080 \pm 0.0018 \text{ mm}$
<i>Mechanical properties</i>	
Tensile test	Tensile strength
	Elongation at break
	Young's modulus
Puncture test	Force at break
	Elongation at break
Barrier properties	Water permeability
	Oxygen permeability (25 °C)
<i>Optical properties</i>	
Color parameters	$L^*(L_s^* = 93.83)$
	$a^*(a_s^* = -0.86)$
	$b^*(b_s^* = 0.86)$
	$\Delta E^*$
	Opacity (Y)
Solubility (g/100 g de M.S.), $T = 25^\circ\text{C}$	$15.90 \pm 0.09$
Water content of QSF (g water/100 g solids)	11.25

Quinoa starch films were conditioned at 25 °C and 58% of relative humidity.

**Table 4**

Some properties of films.

Material – film (starch content/glycerol content)	Film thickness (μm)	Stress at break (MPa)	Elongation at break (%)	O <sub>2</sub> permeability (cm <sup>3</sup> m <sup>-1</sup> s <sup>-1</sup> Pa <sup>-1</sup> )	Water permeability (g m <sup>-1</sup> s <sup>-1</sup> Pa <sup>-1</sup> )	Solubility (%)
Corn starch (34.4%) <sup>a</sup>	104.34			4.61 × 10 <sup>10</sup>	2.57 × 10 <sup>-10</sup>	
Amylomaize (34.4%) <sup>a</sup>	128.7			3.21 × 10 <sup>10</sup>	2.14 × 10 <sup>10</sup>	
Yam starch (33.4%) <sup>b,c</sup>	110	4.70	47	–	1.54 × 10 <sup>-10</sup>	
Yam starch (40%) <sup>b,c</sup>	70	7.84	10.3		1.29 × 10 <sup>-10</sup>	
Yam starch (60%) <sup>b,c</sup>	110	2.84	34.5		1.51 × 10 <sup>-10</sup>	
Amaranth flour (22.5%) <sup>d</sup>	83	1.45	83.74	6.5 × 10 <sup>-13</sup>	8.3 × 10 <sup>-11</sup>	42.25
Amaranth flour <sup>stearic acid/glycerol</sup> (26%) <sup>e</sup>	85–100	2.60	148	2.36 × 10 <sup>-13</sup>	8.9 × 10 <sup>-11</sup>	15.20
Quinoa starch (21.2%) <sup>f</sup>	80	7.56	58.14	0.50 × 10 <sup>-13</sup>	5.6 × 10 <sup>-11</sup>	15.90

<sup>a</sup> Garcia et al. (2000).<sup>b</sup> Mali et al. (2002).<sup>c</sup> Mali, Grossmann, et al. (2005) and Mali, Sakanaka, et al. (2005).<sup>d</sup> Tapia-Blácido et al. (2005).<sup>e</sup> Colla et al. (2006), Amaranth flour films with addition of optimized concentrations of stearic acid (10 g/100 g of amaranth flour) and glycerol (26 g/100 g of amaranth flour).<sup>f</sup> This work.

ited a value for solubility (15.90%) similar to that of the amaranth film (15.20%) produced by Colla et al. (2006), but lower than that of the amaranth film produced by Tapia-Blácido et al. (2005). Certainly, these raw materials were *crude starches*, obtained using a long contact time with an alkaline solution, and probably with a high injury level of the amaranth starch granule, provoking a less compact structured matrix than that of the quinoa starch films, and resulting in higher values for the barrier properties as compared to the QSF. In order to provide an additional water vapor barrier to the amaranth films, Colla et al. (2006) also added stearic acid and glycerol to the polymeric matrix, at concentrations of 10 and 26 g/100 g of flour, respectively. As a consequence they obtained improved values for elongation at break and stress at break and also for the oxygen barrier properties, although the WVP value obtained was lower than that obtained for the amaranth film produced with just the addition of glycerol (Tapia-Blácido et al., 2005). The best results obtained by the QSF can be seen in Tables 3 and 4, but it must be pointed out that the QSF was prepared from the quinoa starch without subsequent chemical treatment and only glycerol was added as a plasticizer, without the addition of any other component or chemical treatment. Based on the results obtained in the present study, it can be seen that all the QSF obtained from the experimental design and also that obtained using the optimized conditions, presented better results. This was probably due to the following: (1) the extraction method used to obtain the quinoa starch, applying the technique of short-time contact with the alkaline solution developed by Araujo-Farro (2008), which decreased starch granule injury and prior denaturation of the protein, (2) the QSF film preparation process used, and (3) the formation of AL and AML during the alkaline-thermal treatment. These results were consistent with those found by Van Soest et al. (1996).

## 6. Conclusions

Quinoa starch appears to be a very interesting raw material for the preparation of edible films and coatings. The process developed here produced colorless films with good mechanical properties and excellent barrier properties. As usual, the glycerol content was the most important parameter influencing the mechanical properties, due to its plasticizing effects on the biopolymer matrix, followed by the effects of the drying conditions and pH value. The combined effects of these variables conferred distinguished physical properties on the QSF as compared to other starch films reported in the specialized literature. The statistical methodology used determined

the following optimal conditions for use in the casting process: 21.2% glycerol, alkaline pH value of 10.7 and drying conditions of 36 °C/14 h.

## Acknowledgements

The authors are grateful to The Brazilian National Council (CAPES) for their financial support and for the research fellowship awarded to Patricia Cecilia Araujo Farro during her studies at the State University of Campinas (Ph.D. Food Engineering Program) (CAPES/PEC-PG program).

## References

- Ahamed, T. N., Singhal, R. S., Kulkarni, P. R., Kale, D. D., & Pal, M. (1996). Studies on *Chenopodium quinoa* and *Amaranthus paniculatus* starch as biodegradable fillers in LDPE films. *Carbohydrate Polymers*, 31, 157–160.
- Alcantara, C. R., Rumsey, T. R., & Krotcha, J. M. (1998). Drying rate effect on the properties of whey protein films. *Journal of Food Process. Eng.*, 21, 387–405.
- AOAC. (1995). *Association of Official Analytical Chemist: Official Methods of Analysis*, 16th ed. Washington, D.C.
- Araujo-Farro, P. C. (2008). Development and optimization of biodegradable films made of products derived from “Royal” variety quinoa (*Chenopodium quinoa* Willdenow) seeds. PhD Thesis. Unicamp. Brazil, p. 303.
- Araujo-Farro, P. C., Podadera, G., Sobral, J. P. A., & Menegalli, F. C. (2006). Development of edible films based on Quinoa (*Chenopodium Quinoa* Willdenow) In *IUFOST 2006/913*, 2006, Nantes. France 13 th World Congress of Food Science and Technology.
- ASTM. (1989). Designation D 3985-81: Standard test method for gas transmission rate of plastic film and sheeting. In *Annual Book of ASTM Standards*. Philadelphia: American Society for Testing and Materials.
- ASTM. (1995). Designation E96-95: Standard method for water vapor transmission of materials. In *Annual Book of ASTM Standards*. Philadelphia: American Society for Testing and Materials.
- ASTM. (1997). Designation D 882-97: Standard test method for tensile properties of thin plastic sheeting. In *Annual Book of ASTM Standards*. Philadelphia: American Society for Testing and Materials.
- Averous, L., & Boquillon, N. (2004). Biocomposites based on plasticized starch: Thermal and mechanical behaviors. *Carbohydrate Polymers*, 56, 111–122.
- Bader, H. G., & Goritz, D. (1994). Investigations on high amylose corn starch films. Part 3: Stress strain behaviour. *Starch/Stärke*, 46(11), 435–439.
- Colla, E., Sobral, P. J. A., & Menegalli, F. C. (2006). Amaranth *cruentus* flour edible films: Influence of stearic acid addition, plasticizer concentration, and emulsion stirring speed on water vapor permeability and mechanical properties. *Journal of Agricultural and Food Chemistry*, 54, 6645–6653.
- Follain, N., Joly, C., Dole, P., & Bliard, C. (2005). Mechanical properties of starch-based materials. I. Short review and complementary experimental analysis. *Journal of Applied Polymer Science*, 97, 1783–1794.
- Garcia, M., Martino, M., & Zaritzky, N. (2000). Microstructural characterization of plasticized starch-based films. *Starch/Stärke*, 52(4), 118–124.
- Gennadios, A., Weller, C. L., Handa, M. A., & Froning, G. W. (1996). Mechanical properties of egg albumen films. *Journal of Food Science*, 61(3), 585–589.

- Guilbert, S. (2000). Edible films and coatings and biodegradable packaging. *Bulletin of the International Dairy Federation*, 346, 10–16.
- Gontard, N., Duchez, C., Cuq, J., & Guilbert, S. (1994). Edible composite films of wheat gluten and lipids: Water vapor permeability and other physical properties. *International Journal Food Science Technology*, 29, 39–50.
- Gontard, N., Guilbert, S., & Cuq, J. L. (1993). Water and glycerol as plasticizers affect mechanical and water vapor barrier properties of an edible wheat gluten film. *Journal of Food Science, Chicago*, 58(1), 206–211.
- Jangchud, A., & Chinnan, M. S. (1999). Peanut protein film as affected by drying temperature and pH of film forming solution. *Journal of Food Science*, 64, 153–157.
- Juliano, B. O. (1971). A simplified assay for milled-rice amylose. *Cereal Science Today*, 16(10), 334–340.
- Khuri, A. J., & Cornell, F. A. (1996). *Response surfaces: Design and analyses* (second ed.). NY: Marcel Dekker.
- Lourdun, D., Della Valle, G., & Colonna, P. (1995). Influence of amylose content on starch films and foams. *Carbohydrate Polymers*, 27, 261–270.
- Mali, S., Grossmann, M. V. E., García, M. A., Martino, M. N., & Zaritzky, N. E. (2002). Microstructural characterization of yam starch films. *Carbohydrate Polymers*, 50, 379–386.
- Mali, S., Grossmann, M. V. E., García, M. A., Martino, M. N., & Zaritzky, N. E. (2005). Mechanical and thermal properties of yam starch films. *Food Hydrocolloids*, 19, 157–164.
- Mali, S., Sakanaka, L. S., Yamashita, F., & Grossmann, M. V. E. (2005). Water sorption and mechanical properties of cassava starch films and their relation to plasticizing effect. *Carbohydrate Polymers*, 60, 283–289.
- Martinez, C., & Cuevas, F. (1989). Evaluación de la calidad culinaria y molinaria del arroz. Guía de estudio. Cali, CIAT, 75.
- Muller, C. M. O., Yamashita, F., & Borges Laurindo, J. (2008). Evaluation of the effects of glycerol and sorbitol concentration and water activity on the water barrier properties of cassava starch films through a solubility approach. *Carbohydrate Polymers*, 72, 82–87.
- Myllärinen, P., Partanen, R., Seppälä, J., & Forsell, P. (2002). Effect of glycerol on behaviour of amylose and amylopectine films. *Carbohydrate Polymers*, 50, 355–361.
- Parris, N., Dickey, L. C., Kurantz, M. J., Moten, R. O., & Craig, J. C. (1997). Water vapor permeability and solubility of Zein/Starch hydrophilic films prepared from dry Milled Corn Extract. *Journal of Food Engineering*, 32, 199–207.
- Perez-Gago, M. B., & Krotcha, J. M. (2000). Drying temperature effect on water vapor permeability and mechanical properties of whey protein–lipid emulsion films. *Journal Agriculture Food Chemistry*, 48, 2687–2692.
- Rooney, L. W., & Suhendro, E. L. (1999). Perspectives on nixtamalisation (alkaline cooking) of maize for tortillas and snack. *Cereal Foods World*, 44, 466–470.
- Sobral, P. J. A., Menegalli, F. C., Hubinger, M., & Roques, M. A. (2001). Mechanical, water vapor barrier and thermal properties of gelatin based edible films. *Food Hydrocolloids*, 15, 423–432.
- Sothornvit, R., & Krotcha, J. M. (2001). Plasticizer effect on mechanical properties of  $\beta$ -lactoglobulin films. *Journal of Food Engineering*, 50, 149–155.
- Tapia-Blácido, D., Sobral, P. J. A., & Menegalli, F. C. (2005). Development and characterization of edible films based on amaranth flour (*Amaranthus caudatus*). *Journal of Food Engineering*, 67, 215–223.
- Vanin, F. M., Sobral, P. J. A., Menegalli, F. C., Carvalho, R. A., & Habitante, A. M. Q. B. (2005). Effects of plasticizers and their concentrations on thermal and functional properties of gelatin based films. *Food Hydrocolloids*, 19, 899–907.
- Van Soest, J. J. G., Hulleman, S. H. D., Wit, D., & Vliegentsart, J. F. G. (1996). Crystallinity in starch bioplastics. *Industry Crop Production*, 5, 11–22.